

Stability and deformation of geosynthetic reinforced soil retaining wall

M.Hyodo, D.Jamalludin, H.Matsuoka, Y.Nakata & H. Murata
 Department of Civil Engineering, Yamaguchi University, Japan

T.Konami
 Okasan Co., Ltd, Japan

J.Nishimura
 Mitsui Sekka Sanshi Co., Ltd, Japan

ABSTRACT : This paper presents the results of a study to evaluate the displacement of a reinforced earth wall using a small model. The study involved two kinds of geosynthetic strips namely rubber and high density polyethylene (HDPE). A series of tests was performed using a moving wall model where strips reinforcement of width 50mm with varying lengths of 300mm, 400mm and 500mm could be tested in dry Aio sand. The results indicate that the wall displacement was greatly influenced by the tensile stiffness of the reinforcement. Furthermore, the strains measured along the strip provide useful information on the behavior of the strip when subjected to, firstly active force and later an additional pull-out force.

1 INTRODUCTION

Reinforced earth walls began to be used widely during the early 1970 's when, firstly steel strips and more recently geosynthetics have been included in the construction of reinforced earth walls and steep slopes. The usage of geosynthetics is made possible due to the production of high strength fibers and polymer mesh which can withstand corrosion and chemical attack when placed in soil. The structure of a reinforced earth wall is simple and because of this, it takes shorter time and is cheaper to construct (Mitchell et al. 1987). Since the tensile stiffness of the geosynthetic is lower than steel, it elongates considerably under tensile forces causing problems of displacement to retaining walls.

2 SPECIFICATIONS FOR G.R.S (GEOSYNTHETIC REINFORCED SOIL) RETAINING WALL MODEL TEST

2.1 Testing apparatus, samples and test conditions

The typical arrangement for the testing apparatus is shown in Fig. 1 and its dimensions are 600mm long by 300mm wide by 450mm high. Acrylic board 10mm thick was used for the wall of the apparatus in order to know the behavior of the reinforced earth wall. The wall was hinged at its bottom so that it could

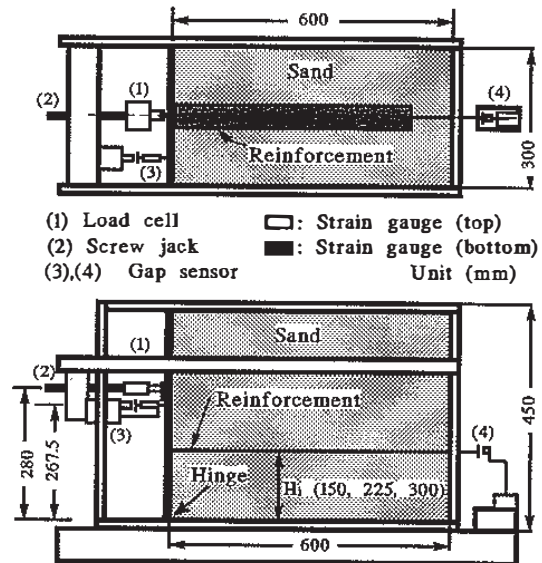


Fig. 1. Typical arrangement of the testing apparatus

move freely and the top of the wall was initially supported by a screw jack. The front portion of the jack had a roller. When the wall acted independently, there was gap between the roller and wall. At the front of the wall, there was hook and when the wall becomes independent, the jack can pull the wall. Dry Aio sand was used as the backfilling material ($G_s=2.62$, $D_{max}=2.0$, $\phi=43.9^\circ$ and $D_r=50\%$). Rubber and high density polyethylene (HDPE) were used as

the reinforcement. Fine Toyoura sand was glued to the surface of the reinforcement so that the reinforcement had a uniform surface roughness. Table 1 shows the tensile stiffness of the reinforcement used and the condition of tests being performed.

Table 1. Summary of the tensile stiffness of the reinforcement used and condition of tests being performed.

Sand	Reinforcement	Width B=50mm	Wall height (mm)
		Length L=500mm	
Tensile stiffness		E*(KN/m)	
Aio sand Dr=50%	(R1)	7.18	300
			375
			450
	(R2)	15.0	200
			250
			300
			375
			450
			450
	(R3)	23.0	200
			250
			300
			375
			450
			450
(HDPE)	333.0	200	
		250	
		300	
		375	
		450	
		450	

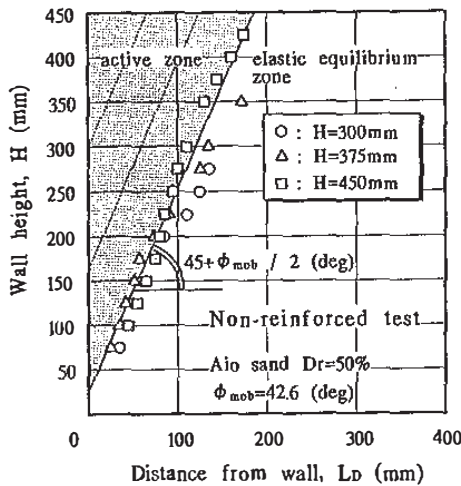


Fig. 2. The failure plane of non-reinforced wall

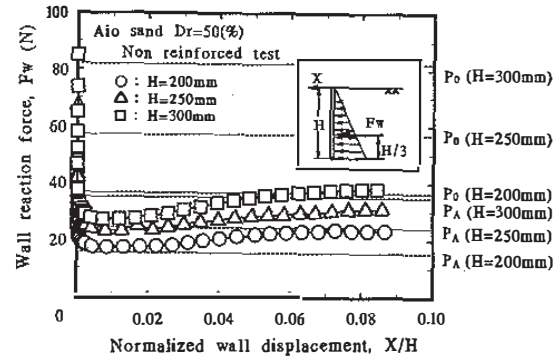


Fig. 3. The relationship of wall reaction force against normalized wall displacement for non-reinforced wall

2.2 Test procedure

a. The wall was held in a vertical position by the screw jack in front of it. Sand was placed in 25mm layers until to the reinforcement level.

b. The reinforcement was fixed to the wall and sand was further filled to the required height. It was left for about one hour.

c. The jack was then pulled at a rate of 0.3mm/minute and the measurements of reaction force on the jack, front displacement of wall, end displacement of the reinforcement and strain along the reinforcement were taken.

d. Once the wall became independent, the wall was then pulled.

3 TEST RESULTS AND CONSIDERATIONS

3.1 Earth pressure and wall displacement

3.1.1 Non-reinforced wall

In the case of the non-reinforced wall, the wall did not become independent but a failure plane as shown in Fig. 2 occurred. Using Rankine's formula and by doing back calculation, the angle of shearing resistance of the sand was found to be $\phi = 42.6^\circ$. This value is in close agreement with that found using triaxial tests. Fig. 3 shows the wall force (F_w) against normalized wall displacement (X/H) with varying height of sand. It can be seen that, for a very small displacement, that is between $X/H=0.001$ and $X/H=0.002$, the wall force changes from a force at rest to an active force (Murata et al. 1995). From the normalized wall displacement of $X/H=0.04$ onward,

the value of F_W increased since the weight of soil was acting on the inclined wall.

3.1.2 Reinforced wall

Fig. 4 shows the relationship of wall reaction force F_W to normalized wall displacement (X/H). The black circle markers represent the results for a non-reinforced wall. Beyond $X/H=0.002$, the value of F_W remains constant and it represents the value of the active force P_A . In the case of the reinforced wall, the value of F_W decreases to zero as the wall displacement increases and from this moment onwards, the wall became independent of the jack. This means that the active force was completely taken by the tensile force of the reinforcement. The higher the value of the tensile stiffness of the reinforcement, the smaller is the wall displacement for the wall to become independent (Murata et al. 1995).

In the process of the wall becoming independent, the front tensile force of the reinforcement (T_R) can be calculated by using the following equation:

$$T_R = \frac{(P_A - F_W) \times H_D}{H_i} \quad (1)$$

where P_A is the active earth force, H_D is the centre of active force from bottom, H_i is the height of the reinforcement from bottom and F_W is the wall reaction force. When the wall becomes independent of the jack, $F_W=0$ and $T_R=T_{RS}$, then equation 1 becomes as follows:

$$T_{RS} = \frac{P_A \times H_D}{H_i} \quad (2-a)$$

After the wall becomes independent and is subjected to pull-out force, the value of T_R is as follows:

$$T_R = T_{RS} + \frac{F_P \times H_j}{H_i} \quad (2-b)$$

where F_P is the pulling force and H_j is the height of the pulling point from bottom. Table 2 shows the front tensile forces when the walls become independent for the reinforced walls with various wall heights. They were calculated by substituting the measured active force P_A into equation 2-a.

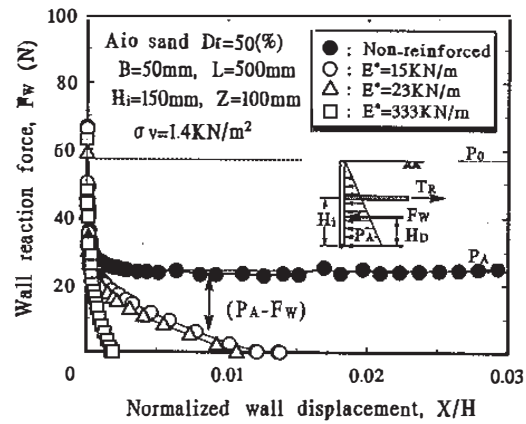


Fig. 4. Relationship of wall reaction force against normalized wall displacement for reinforced wall

Table 2. Correlation of the wall heights, active forces and front tensile forces of the reinforcement when walls become independent for reinforced wall.

Sand	Wall height H (mm)	Overburden pressure, σ_v (KN/m ²)	Force at rest, P_o (N)	Active force, P_A (N)	T_{RS} (N)
Aio sand	200	0.7	36.4	15.76	7.0
	250	1.4	66.9	25.20	14.0
	300	2.1	81.9	31.50	21.0
	375	3.5	128.0	41.88	34.9
	450	4.2	184.3	64.87	65.2

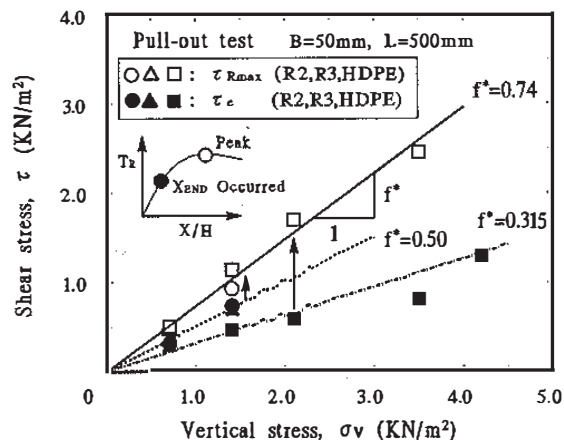


Fig. 5. Shear stress on the reinforcement against vertical stress

3.2 Pull-out resistance

Fig. 5 shows the relationship between shear stress and overburden pressure. τ_c is the shear stress when the end of the reinforcement started to move and is shown by all the black markers as in Fig. 5. The

maximum shear stress τ_{Rmax} (\circ , \triangle and \square) is the shear stress when the maximum front tensile force of the reinforcement occurred. The shear stress can be calculated using the following formula:

$$\tau = \frac{T_R}{2 \times B \times L} \quad (3)$$

where B is the breadth and L is the length of the reinforcement.

From this figure, the relationship between shear stress and overburden pressure can be shown by a straight line where the gradient represents the value of apparent coefficient of friction (f'). At the peak of tensile force (\circ , \triangle , \square), the value of the apparent coefficient of friction $f' = 0.74$ and it is independent of the tensile stiffness (E^*) of the reinforcement (Fang, 1991). When the end portion of the reinforcement started to move, it was observed that, for a higher value of tensile stiffness (\blacksquare , $E^* = 333\text{KN/m}$), the value of coefficient of friction is smaller than for material having a lower tensile stiffness (\bullet , $E^* = 15\text{KN/m}$ and \blacktriangle , $E^* = 23\text{KN/m}$).

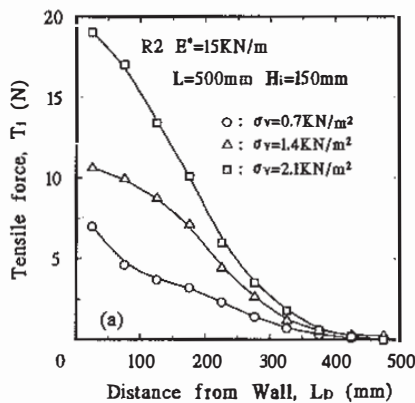


Fig. 6a. Tensile force distribution along the reinforcement (influence of the overburden pressure)

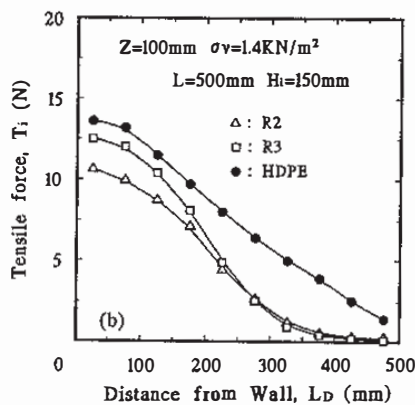


Fig. 6b. Tensile force distribution along the reinforcement (influence of the tensile stiffness)

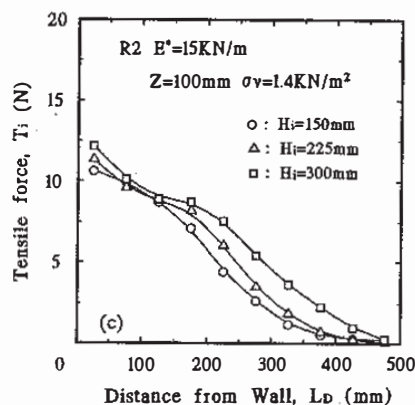


Fig. 6c. Tensile force distribution along the reinforcement (influence of the height of the reinforcement from bottom)

3.3 Distribution of tensile force along the reinforcement and its transmission characteristic

Fig. 6a is the tensile distribution along the reinforcement when the wall becomes independent with varying overburden pressure, $z = 50, 100$ and 150mm . The transmission of tensile force along the reinforcement is dependent on the overburden pressure. Friction at any point along the reinforcement can be found using equation 3. Since the value of $1/2B$ is constant, the friction is proportional to $\delta T / \delta L$ (curve gradient). Fig. 6b is the distribution of tensile force along the reinforcement when wall becomes independent for reinforcements of different tensile stiffness. At the distance from wall $L_D = 25 \sim 75\text{mm}$, the friction is zero since the curves are almost horizontal ($\delta T / \delta L = 0$). From Fig. 2, the zone between $L_D = 25 \sim 75\text{mm}$, is located in the active zone and it can be concluded that the friction is zero in this region. In the case of HDPE ($E^* = 333\text{KN/m}$), the reinforcement acts as if it is a rigid material with friction almost uniformly mobilized and the value of $\delta T / \delta L$ constant along the reinforcement (Schlosser et al. 1978). In the case of R2 ($E^* = 15\text{KN/m}$) and R3 ($E^* = 23\text{KN/cm}$), deformation of the reinforcement predominates with a large friction at the front and gradually reduces as the distance from the wall increases (Schlosser et al. 1978).

Fig. 6c shows the graphs of tensile force distribution along the reinforcement with varying

height of reinforcement from the bottom ($H_i=150, 225$ and 300mm). The front most tensile forces for $H_i=225$ (\triangle) and 300mm (\square), are slightly higher than expected due to the front portion of the reinforcements being bent as the wall moved. From Fig. 2, as the value of H_i increases, the zone of zero friction (active zone) increases. Beyond $L_D=150\text{mm}$, the friction is the same and it is independent of H_i .

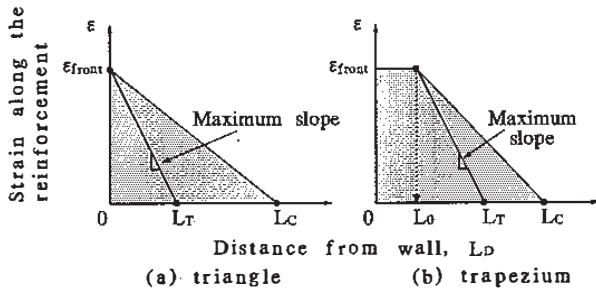


Fig. 7. Idealized shape of the strain distribution along the reinforcement

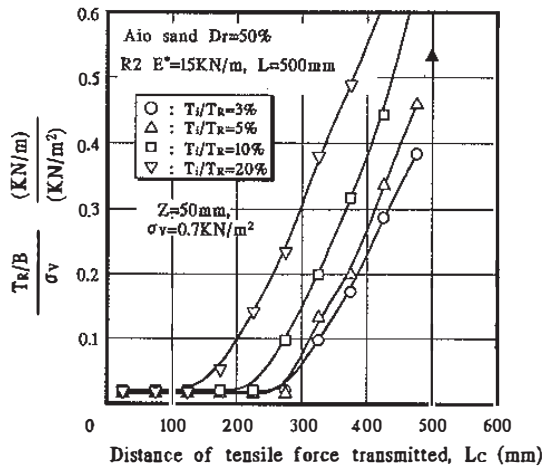


Fig. 8. Characteristic of the tensile force transmission when $T_i/T_R = 3\sim 20\%$

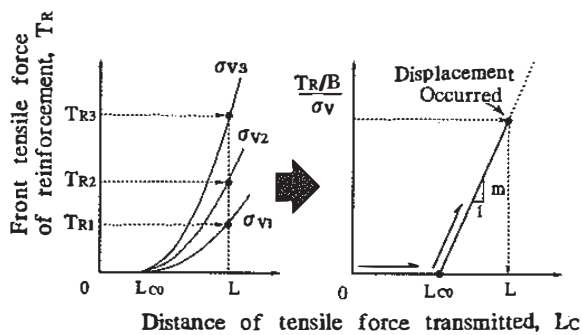


Fig. 9. Modelling of the tensile force transmission

4 EVALUATION OF DEFORMATION OF G.R.S. RETAINING WALL MODEL TEST

4.1 Evaluation method

The wall displacement δ can be evaluated using the following equation:

$$\delta = \int_0^{L_{Re}} \varepsilon_i(L) \cdot dL \quad (4)$$

where δ is wall displacement, $\varepsilon_i(L)$ is the strain distribution and L_{Re} is the effective friction length. To evaluate δ using equation 4, it is necessary to evaluate the strain distribution and the effective friction length. It is assumed that L_{Re} is the distance from the wall to a position where T_R is very small (almost zero). It is already known from the series of tests completed, that the shape of the strain distribution is either a triangle or a trapezium. Fig. 7 shows the assumption of strain distribution in this study. In the case of a trapezoidal shaped strain distribution, L_0 is the boundary between the active zone and the elastic equilibrium zone. The value of L_T can be calculated from equation 5 as follows:

$$L_T = \frac{T_R}{2 \times B \times \sigma_v \times f'} \quad (5)$$

where T_R is the front tensile force of the reinforcement, B is the width of the reinforcement, and σ_v is the overburden pressure. The value of f' is the apparent coefficient of friction when the end displacement of the reinforcement started to occur. By using equation 4, the wall displacements δ_c and δ_T are calculated using L_c and L_T , respectively. The value of δ_c is considered as the upper limit of predicted elongation of reinforcement while the lower limit of predicted elongation of reinforcement is considered as δ_T . It can be seen that the experimental strain distribution is located between the predicted upper and lower limits of strain distribution.

4.2 Determination of parameters

Using equation 4, the material elongation can be obtained. The value of L_{Re} has to be decided first. Fig. 8 shows the relationship between $T_R/B/\sigma_v$ and L_c when the tensile force ratio T_i/T_R reached $3\sim 20\%$.

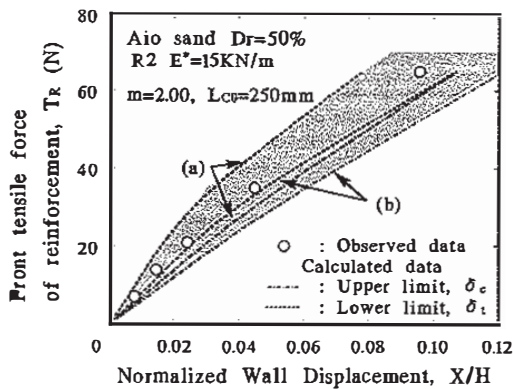


Fig. 10. Relationship between tensile force of the reinforcement and normalized wall displacement (comparison between observed and calculated data)

The value of T_i/T_R is the ratio of the internal tensile force along the reinforcement to the front tensile force of the reinforcement.

The black triangle marker indicates the point when the end displacement of the reinforcement started to happen. In this figure, when a very small tensile force was applied to the front of the reinforcement, the tensile force was transmitted through the reinforcement to about 20cm from the wall. Beyond 20cm from the wall, the relationship between $T_R/B/\sigma_v$ and L_C can be shown as a straight line and it is independent of the value T_i/T_R . The black triangle marker lies on the line $T_i/T_R = 5\%$. This line can be considered as a boundary line when slippage of the reinforcement started to occur. In this study, the distance from wall (parallel to L_C axis line) to any point on the line $T_i/T_R = 5\%$ represents the point of L_C . Fig. 9 shows the modelling of the tensile force transmission characteristic. The relationship between T_R and L_C under any value of overburden pressure can be evaluated if values of L_{C_0} and m are known where L_{C_0} is the initial distance of tensile force transmission while m is the gradient of the boundary line (line $T_i/T_R = 5\%$).

4.3 Application for G.R.S retaining wall model test

Fig. 10 shows a comparison between the experimental and predicted results of wall displacement when the wall becomes independent. It can be seen that the experimental data lie between δ_c and δ_t . It was also found that the wall

displacement could be predicted accurately using this method. The predicted results using a trapezoidal shaped strain distribution and values of L_C are in a close agreement with the experimental results.

5 CONCLUSIONS

The higher the tensile stiffness of the reinforcement, the smaller is the wall displacement for full transfer of active force to the reinforcement.

The transmission of the tensile force along the reinforcement is dependent on the tensile stiffness of the reinforcement. For reinforcement with higher value of tensile stiffness, friction is uniformly mobilized along the reinforcement while for material with lower tensile stiffness, deformation predominates with greatest friction at the front and gradually reduces as the distance from wall increases.

It is possible to evaluate accurately the experimental wall displacement from the model presented. The model presented idealized the transmission of tensile force along the reinforcement and also idealized the shape of tensile force distribution along the reinforcement

REFERENCES

- Fang, H. Y. 1991. *Foundation Engineering Handbook* : 778-795. New York : Van Nostrand Reinhold.
- Mitchell, J.K., Villet, W.C.B. 1987. Reinforcement of Earth Slopes and Embankments, *National Cooperative Highway Research Program Report 290*, Transport Research Board, National Research Council
- Murata, H., Hyodo, M., Yamamoto, O., Matsuoka, H., Konami, T. 1995. Tensile stiffness of belt-type reinforcement and movement of retaining wall: *Proc. 30th. Symp. JSSMFE* : 2439-2440. (in Japanese)
- Schlosser, F., Elias, V. 1978. Friction in reinforced earth, *Symp. on earth reinforcement*: 735-763. ASCE.